Appl. Math. Mech. -Engl. Ed., **38**(11), 1551–1564 (2017)
DOI 10.1007/s10483-017-2278-9

Applied Mathematics and Mechanics (English Edition)

Model predictive control of rigid spacecraft with two variable speed control moment gyroscopes*

Pengcheng WU, Hao WEN†, Ti CHEN, Dongping JIN

State Key Laboratory of Mechanics and Control of Mechanical Structures, Nanjing University of Aeronautics and Astronautics, Nanjing 210016, China

Abstract In this paper, an attitude maneuver control problem is investigated for a rigid spacecraft using an array of two variable speed control moment gyroscopes (VSCMGs) with gimbal axes skewed to each other. A mathematical model is constructed by taking the spacecraft and the gyroscopes together as an integrated system, with the coupling interaction between them considered. To overcome the singular issues of the VSCMGs due to the conventional torque-based method, the first-order derivative of gimbal rates and the second-order derivative of the rotor spinning velocity, instead of the gyroscope torques, are taken as input variables. Moreover, taking external disturbances into account, a feedback control law is designed for the system based on a method of nonlinear model predictive control (NMPC). The attitude maneuver can be realized fast and smoothly by using the proposed controller in this paper.

Key words integrated system, variable speed control moment gyroscope (VSCMG), nonlinear model predictive control (NMPC)

Chinese Library Classification O313.3
2010 Mathematics Subject Classification 70E17, 70K99, 70Q05

1 Introduction

Control moment gyroscopes (CMGs) obtain the angular momentum via high speed spinning rotor, and export torques owing to the change of angular momentum. CMGs are widely used in large spacecrafts due to their merits of producing larger torques, having simpler physical structure, longer life span, higher precision, and higher stability than conventional flywheels or jets[1–2].

Currently, CMGs are mainly divided into some sorts according to their structures, such as single gimbal control moment gyroscopes (SGCMGs) and variable speed control moment gyroscopes (VSCMGs). An SGCMG holds the constant rotor spinning velocity and produces output torque on account of the change of angular momentum caused by the rotation of gimbal axis. The SGCMG has a simple structure and large torque amplification ability, and is widely used in the field of spacecraft control. However, an SGCMG can only produce gyroscope torque in one direction. In order to realize three axes control of the spacecraft, more than three SGCMGs are needed[3]. In addition, the configuration of SGCMGs is usually designed to be

* Received Nov. 10, 2016 / Revised May 24, 2017
Project supported by the National Natural Science Foundation of China (Nos. 11372130, 11290153, and 11290154)
† Corresponding author, E-mail: wenhao@nuaa.edu.cn

redundant to keep the system from unexpected failures caused by the breakdown of SGCMGs. For instance, Chinese 'Tiangong-1' space station is configured with six SGCMGs[4]. Moreover, the SGCMG has a singularity problem[5]. Inevitably, there are some combinations of gimbal angles such that SGCMGs cannot produce demanded torques[6]. For the design redundancy, many steering laws have been used such as the Moore-Penrose pseudo-inverse steering law. However, these steering laws cannot make the system escape from singular states[7]. Faced with this problem, many researchers designed various improved steering laws such as singularity robust inverse (SRI) and pseudo-inverse with null motion. Nevertheless, as far as we know, no simple and effective steering law can solve the singularity problem completely.

In contrast, reaction wheels (RWs) can produce output torques owing to the variation of the spinning rates of rotors. Different from that, VSCMGs have both the features of RWs and SGCMGs. While the rotor spinning rate of the SGCMG remains constant, the rotor spinning rate of the VSCMG is allowed to vary in a continuous manner. Therefore, a VSCMG can produce output torque by virtue of the rotation of gimbal axis and change of rotor spinning rate. Since a VSCMG has an extra degree of freedom, its structure will be more complex compared with SGCMGs. Ford and Hall[8] introduced the equations of motion of a spacecraft which contained several VSCMGs. However, the RW and CMG modes were operated exclusively, not simultaneously in their control laws. Schaub et al.[9] designed control laws which can change modes of RW and CMG automatically in their paper. Schaub and Junkins[10] also proposed steering laws with null motion, which can make VSCMGs escape from singular configuration under the circumstance of generating no output torques. Cui and He[11] designed steering laws for two parallel VSCMGs. Kanzawa et al.[12] proposed steering laws which not only provide the demanded control torques, but also control the terminal gimbal angles of CMGs.

The spacecraft and the array of CMGs were usually studied independently in the recent relevant literature. Firstly, the control torques needed by a spacecraft are designed, and then steering laws are obtained by solving the gimbal rates and rotor spinning accelerations of CMGs according to the reference control torques. The actual torques produced by CMGs are not precisely equal to the demanded torques due to the possible singularity. It is pointed out here that CMGs are treated as ideal actuators where the interaction between the array of CMGs and spacecraft is ignored. By treating gimbal rates as input variables and considering the spacecraft and the array of CMGs as a whole system, Bhat and Tiwari[13] built a mathematical model which was used to avoid the effect of singularity, without considering the influence of external disturbances on the system in their paper. By taking external disturbances into account, the method of nonlinear model predictive control (NMPC) was used to implement the attitude feedback control of the integrated system of spacecraft and the array of SGCMGs[14]. The dynamics of the coupling system consisting of the array of VSCMGs and spacecraft has not been considered in those studies above, where SGCMGs were only used as actuators.

Generally, CMGs are configured in a spacecraft redundantly to obtain torques along three independent directions. However, some uncertainties, such as mechanical malfunctions, may cause the onboard failures of CMGs. Therefore, CMGs with gimbal axes skewed to each other seem to be the better choice serving as actuators[15]. Many researchers intensively investigated the attitude control problem of those systems. For example, Crouch[16] discussed the controllability of a system which was driven by flywheels, and concluded that the system with less than three flywheels can never become controllable. Hu and Ge[17] developed a control law for spacecrafts driven by jets. Yang and Wu[18] considered the orientation control of a spacecraft driven by arbitrary configurations of double SGCMGs. Bhat and Tiwari[13] showed that with one or more CMGs, the combined dynamics of the spacecraft-CMG system was globally controllable, despite the presence of singularity. Gui et al.[15] designed a controller by reducing the kinematic and dynamic equations of a spacecraft driven by two SGCMGs with gimbal axes skewed to each other. Flywheels, jets, and SGCMGs were mostly used as actuators in those studies above.

In this paper, the attitude maneuver control problem of a rigid spacecraft via the array of VSCMGs is investigated. Firstly, the strategy is developed on how to drive the rigid spacecraft into the desired attitude when unexpected failures of CMGs occur during the operation. Next, the spacecraft and VSCMGs are taken as a whole system, and the coupling interaction between the spacecraft and VSCMGs is considered. Different from the conventional methods where steering laws are proposed to drive CMGs, the first-order derivative of gimbal rates and the second-order derivative of the rotor spinning velocity are treated directly as input variables in this paper, and the singularity problem will not be present any more. At last, the attitude maneuver control law for the spacecraft is designed based on the NMPC. The remaining part of this paper is organized as follows. In Section 2, the integrated system of spacecraft and the array of VSCMG is built. In Section 3, the control task is formulated, and the controller based on the NMPC method is designed. In Section 4, a simulation case is given, and the feasibility of the proposed controller is verified by numerical simulation. As a comparison, a steering law based on the conventional method is also discussed briefly.

2 Mathematical modeling

In this study, a rigid spacecraft driven by two VSCMGs is considered. The spacecraft and the array of VSCMGs are studied as an entire system.

The total angular momentum of this entire system is

$$\boldsymbol{H} = \boldsymbol{J}\boldsymbol{\omega} + \boldsymbol{h}_{\mathrm{CMG}}, \tag{1}$$

where $\boldsymbol{J}$ represents the inertial matrix of spacecraft, $\boldsymbol{J}\boldsymbol{\omega}$ represents the angular momentum of spacecraft, and $\boldsymbol{h}_{\mathrm{CMG}}$ represents the total angular momentum of VSCMGs. The time derivative of Eq. (1) can be expressed as

$$\dot{\boldsymbol{H}} = \widetilde{\dot{\boldsymbol{H}}} + \boldsymbol{\omega} \times \boldsymbol{H}, \tag{2}$$

where $\widetilde{\dot{\boldsymbol{H}}}$ is the derivative of the angular momentum of system in the spacecraft-fixed frame. $\boldsymbol{\omega}$ represents the angular velocity of spacecraft.

According to the angular momentum theorem[19], one has

$$\dot{\boldsymbol{H}} = \boldsymbol{T}_{\mathrm{ext}}, \tag{3}$$

where $\boldsymbol{T}_{\mathrm{ext}}$ stands for the outer space disturbances. In general, the magnitude of $\boldsymbol{T}_{\mathrm{ext}}$ is very small, about $10^{-7}\,\mathrm{N}\cdot\mathrm{m}$[20].

According to Eqs. (1)–(3), the dynamic equation of spacecraft with CMGs is

$$\boldsymbol{J}\dot{\boldsymbol{\omega}} + \boldsymbol{\omega} \times \boldsymbol{J}\boldsymbol{\omega} = -\widetilde{\dot{\boldsymbol{h}}}_{\mathrm{CMG}} - \boldsymbol{\omega} \times \boldsymbol{h}_{\mathrm{CMG}} + \boldsymbol{T}_{\mathrm{ext}}, \tag{4}$$

where $\widetilde{\dot{\boldsymbol{h}}}_{\mathrm{CMG}}$ stands for the derivative of the angular momentum of the array of CMGs in the spacecraft-fixed frame.

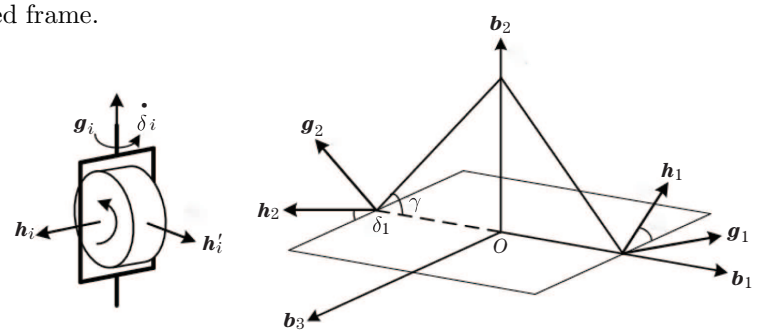

Fig. 1 Schematic configuration of two skew VSCMGs

As shown in Fig. 1, the configuration of two VSCMGs with gimbal axes skewed to each other is the focus of the present study. γ is an oblique angle held constant. Unit orthogonal bases $\{\boldsymbol{b}_1,\ \boldsymbol{b}_2,\ \boldsymbol{b}_3\}$ stand for the spacecraft-fixed frame, while $\boldsymbol{g}_i$ and $\boldsymbol{h}_i$ represent the gimbal axis and the angular momentum of the ith VSCMG, respectively. In fact, $\boldsymbol{h}_i$ is a function of the gimbal angle δ_i and the rotor spinning velocity Ω_i, i.e., $\boldsymbol{h}_i = \boldsymbol{h}_i(\delta_i, \Omega_i)$, where Ω_i determines the magnitude of $\boldsymbol{h}_i$, while δ_i represents the direction of $\boldsymbol{h}_i$. The total angular momentum of the two VSCMGs is

$$\boldsymbol{h}_{\mathrm{CMG}} = \boldsymbol{h}_1(\delta_1, \Omega_1) + \boldsymbol{h}_2(\delta_2, \Omega_2). \tag{5}$$

Let J_{W} denote the moment of inertia of rotor. Hence, the total angular momentum is presented as follows:

$$\begin{aligned}\boldsymbol{h}_{\mathrm{CMG}} &= J_{\mathrm{W}} \begin{bmatrix} -\Omega_1 \sin\delta_1 \cos\gamma \\ \Omega_1 \sin\delta_1 \sin\gamma \\ -\Omega_1 \cos\delta_1 \end{bmatrix} + J_{\mathrm{W}} \begin{bmatrix} \Omega_2 \sin\delta_2 \cos\gamma \\ \Omega_2 \sin\delta_2 \sin\gamma \\ \Omega_2 \cos\delta_2 \end{bmatrix} \\ &= J_{\mathrm{W}} \begin{bmatrix} -\sin\delta_1 \cos\gamma & \sin\delta_2 \cos\gamma \\ \sin\delta_1 \sin\gamma & \sin\delta_2 \sin\gamma \\ -\cos\delta_1 & \cos\delta_2 \end{bmatrix} \begin{bmatrix} \Omega_1 \\ \Omega_2 \end{bmatrix}. \end{aligned} \tag{6}$$

The derivative of Eq. (6) in the spacecraft-fixed reference frame can be expressed as

$$\begin{aligned}\widetilde{\dot{\boldsymbol{h}}}_{\mathrm{CMG}} = {} & J_{\mathrm{W}} \begin{bmatrix} -\cos\gamma \sin\delta_1 \dot{\Omega}_1 \\ \sin\gamma \sin\delta_1 \dot{\Omega}_1 \\ -\dot{\Omega}_1 \cos\delta_1 \end{bmatrix} + J_{\mathrm{W}} \begin{bmatrix} -\cos\gamma \cos\delta_1 \Omega_1 \dot{\delta}_1 \\ \sin\gamma \cos\delta_1 \Omega_1 \dot{\delta}_1 \\ \Omega_1 \sin\delta_1 \dot{\delta}_1 \end{bmatrix} \\ & + J_{\mathrm{W}} \begin{bmatrix} \cos\gamma \sin\delta_2 \dot{\Omega}_2 \\ \sin\gamma \sin\delta_2 \dot{\Omega}_2 \\ \dot{\Omega}_2 \cos\delta_2 \end{bmatrix} + J_{\mathrm{W}} \begin{bmatrix} \cos\gamma \cos\delta_2 \Omega_2 \dot{\delta}_2 \\ \sin\gamma \cos\delta_2 \Omega_2 \dot{\delta}_2 \\ -\Omega_2 \sin\delta_2 \dot{\delta}_2 \end{bmatrix}. \end{aligned} \tag{7}$$

For the sake of notational simplicity, Eq. (7) can be rewritten in the compact form of

$$\widetilde{\dot{\boldsymbol{h}}}_{\mathrm{CMG}} = J_{\mathrm{W}} [\boldsymbol{D}_0 \ \ \boldsymbol{D}_1] \dot{\boldsymbol{\eta}}, \tag{8}$$

where

$$\begin{aligned} \boldsymbol{D}_0 &= \begin{bmatrix} -\cos\gamma \sin\delta_1 & \cos\gamma \sin\delta_2 \\ \sin\gamma \sin\delta_1 & \sin\gamma \sin\delta_2 \\ -\cos\delta_1 & \cos\delta_2 \end{bmatrix}, \\ \boldsymbol{D}_1 &= \begin{bmatrix} -\cos\gamma \cos\delta_1 \Omega_1 & \cos\gamma \cos\delta_2 \Omega_2 \\ \sin\gamma \cos\delta_1 \Omega_1 & \sin\gamma \cos\delta_2 \Omega_2 \\ \sin\delta_1 \Omega_1 & -\Omega_2 \sin\delta_2 \end{bmatrix}, \\ \dot{\boldsymbol{\eta}} &= \begin{bmatrix} \dot{\Omega}_1 & \dot{\Omega}_2 & \dot{\delta}_1 & \dot{\delta}_2 \end{bmatrix}^{\mathrm{T}}. \end{aligned}$$

Hence, Eq. (6) can also be rewritten as

$$\boldsymbol{h}_{\mathrm{CMG}} = J_{\mathrm{W}} \boldsymbol{D}_0 \boldsymbol{\Omega}. \tag{9}$$

Substituting Eqs. (8) and (9) into Eq. (4), the dynamic equation of system is derived in the spacecraft-fixed reference frame,

$$\boldsymbol{J}\dot{\boldsymbol{\omega}} + \boldsymbol{\omega} \times \boldsymbol{J}\omega = -J_{\mathrm{W}} [\boldsymbol{D}_0 \ \ \boldsymbol{D}_1] \dot{\boldsymbol{\eta}} - \boldsymbol{\omega} \times J_{\mathrm{W}} \boldsymbol{D}_0 \boldsymbol{\Omega} + \boldsymbol{T}_{\mathrm{ext}}. \tag{10}$$

In addition, from the perspective of physical significance, one has

$$\boldsymbol{T}_{\mathrm{ctrl}} = -\widetilde{\dot{\boldsymbol{h}}}_{\mathrm{CMG}} = -J_{\mathrm{W}}\left[\boldsymbol{D}_0 \;\; \boldsymbol{D}_1\right]\dot{\boldsymbol{\eta}}, \tag{11}$$

where $\boldsymbol{T}_{\mathrm{ctrl}}$ stands for the output torques produced by the array of VSCMGs.

To describe the attitude of spacecraft in this paper, unit quaternions are used, which were given by[21–22]

$$q_0 = \cos\frac{\theta}{2}, \quad \begin{bmatrix} q_1 \\ q_2 \\ q_3 \end{bmatrix} = \boldsymbol{\varepsilon}\sin\frac{\theta}{2} \tag{12}$$

subject to the constraint

$$q_0^2 + q_1^2 + q_2^2 + q_3^2 = 1. \tag{13}$$

The rotational angle θ is about the Euler axis, which is determined by the unit vector $\boldsymbol{\varepsilon}$.

The kinematic equation of spacecraft is

$$\begin{bmatrix} \dot{q}_0 \\ \dot{q}_1 \\ \dot{q}_2 \\ \dot{q}_3 \end{bmatrix} = \frac{1}{2}\boldsymbol{Q}^{\mathrm{T}}\boldsymbol{\omega}, \tag{14}$$

where

$$\boldsymbol{Q}^{\mathrm{T}} = \begin{bmatrix} -q_1 & -q_2 & -q_3 \\ q_0 & -q_3 & q_2 \\ q_3 & q_0 & -q_1 \\ -q_2 & q_1 & q_0 \end{bmatrix}. \tag{15}$$

3 Controller design

The control task in this section is to drive the spacecraft to the target attitude with the desired angular velocity. The desired attitude and angular velocity are denoted as $\boldsymbol{q}_{\mathrm{f}}$ and $\boldsymbol{\omega}_{\mathrm{f}}$. The objective of the control problem can be formulated as follows:

$$\lim_{t\to\infty}\boldsymbol{q} = \boldsymbol{q}_{\mathrm{f}}, \quad \lim_{t\to\infty}\boldsymbol{\omega} = \boldsymbol{\omega}_{\mathrm{f}}. \tag{16}$$

The spacecraft and the array of CMGs are conventionally studied separately in the previous work. Firstly, the demanded control torques needed by the spacecraft are calculated. Then, the demanded control torques are considered as system input variables, and the steering laws are formulated in order to solve for the gimbal rates and rotor spinning accelerations of CMGs[23]. To compare with the control strategy proposed below in this paper, a conventional method based on the design of steering laws is briefly discussed here in advance.

The array of CMGs usually responds to the demanded torques through certain steering laws. Define the matrix $\boldsymbol{L}$ as $\boldsymbol{L} = [\boldsymbol{D}_0 \;\; \boldsymbol{D}_1]$. Then, a steering law for the array of VSCMGs introduced in Ref. [9] is adopted here,

$$\dot{\boldsymbol{\eta}} = \begin{bmatrix} \dot{\boldsymbol{\Omega}} \\ \dot{\boldsymbol{\delta}} \end{bmatrix} = \frac{1}{J_{\mathrm{W}}}\boldsymbol{W}\boldsymbol{L}^{\mathrm{T}}(\boldsymbol{L}\boldsymbol{W}\boldsymbol{L}^{\mathrm{T}})^{-1}\widetilde{\dot{\boldsymbol{h}}}_{\mathrm{CMG}}, \tag{17}$$

where

$$\boldsymbol{W} = \mathrm{diag}\left[W_{s_1},\ W_{s_2},\ W_{g_1},\ W_{g_2}\right],$$

$$W_{s_i} = W_{s_i}^0 \mathrm{e}^{(-\mu\delta)}, \quad W_{g_i} = \text{const.},$$

$$d = \det\left(\boldsymbol{D}_1 \boldsymbol{D}_1^{\mathrm{T}}\right).$$

In fact, the minimum solution for $\dot{\boldsymbol{\eta}}$ can be figured out through the Moore-Penrose inverse, as the matrix $\boldsymbol{L}$ is never rank deficient. Nevertheless, in order to make VSCMGs act like classical SGCMGs away from singular configurations, a weighted pseudo-inverse is available instead. W_{s_i} and W_{g_i} are the weights relevant to how nearly VSCMGs are to operate like the regular modes of RWs or SGCMGs. To fulfill the desired performance of VSCMGs, the weights are made dependent on the proximity to the singularity of SGCMGs. Besides, for the sake of evaluating the proximity, the scalar d is defined. W_{s_i} and μ are positive scalars chosen by the controller, whereas W_{g_i} simply remains constant.

Different from the conventional method mentioned above, the first-order derivative of gimbal rates and the second-order derivative of rotor spinning velocity can be adopted directly as input variables, and the singularity problem will not be present anymore. Finally, the attitude maneuver control law for the spacecraft can be obtained based on the NMPC method[24–30].

Based on the strategy above, Eq. (4) can be rewritten to obtain the state equations of system as follows:

$$\begin{cases} \dot{\boldsymbol{q}} = \dfrac{1}{2}\boldsymbol{Q}^{\mathrm{T}}\boldsymbol{\omega}, \\ \boldsymbol{J}\dot{\boldsymbol{\omega}} = \boldsymbol{T}_{\mathrm{ext}} - \widetilde{\dot{\boldsymbol{h}}}_{\mathrm{CMG}} - \boldsymbol{\omega} \times \boldsymbol{h}_{\mathrm{CMG}} - \boldsymbol{\omega} \times \boldsymbol{J}\boldsymbol{\omega}, \\ \ddot{\boldsymbol{\delta}} = \boldsymbol{u}, \\ \ddot{\boldsymbol{\Omega}} = \boldsymbol{v}. \end{cases} \tag{18}$$

It is worth noting that though the dynamics of the spacecraft has been added in Eq. (18), the output torques produced by the array of CMGs are not treated as input vectors of the system here. Otherwise, the coupling interaction between the array of CMGs and spacecraft will be ignored, and the actual torques will not be equal to the demanded torques precisely under the circumstance of singularity. Through taking $\dot{\boldsymbol{\delta}}$ and $\dot{\boldsymbol{\Omega}}$ as state variables and $\ddot{\boldsymbol{\delta}}$ and $\ddot{\boldsymbol{\Omega}}$ as system input variables directly, the singularity problem can be converted into an optimal problem with constraints of state and input variables. Hence, the singularity problem is avoided. Accordingly, there is no need to find the inverse mapping from demanded control torques to state variables of CMGs any more. The actual torques will always be equal to the demanded torques precisely.

To ensure the consistency between the model and the real system, the state constraints and input constraints of the system must be taken into consideration. The initial conditions and constraints are mentioned below.

The initial conditions of state variables are

$$\begin{cases} \boldsymbol{q} = \boldsymbol{q}_0, \quad \boldsymbol{\delta} = \boldsymbol{\delta}_0, \quad \boldsymbol{\Omega} = \boldsymbol{\Omega}_0, \\ \boldsymbol{\omega} = \boldsymbol{\omega}_0, \quad \dot{\boldsymbol{\delta}}_0 = \dot{\boldsymbol{\delta}}_0, \quad \dot{\boldsymbol{\Omega}} = \dot{\boldsymbol{\Omega}}_0. \end{cases}$$

The terminal constraints of output variables are

$$\begin{cases} \boldsymbol{q} = \boldsymbol{q}_{\mathrm{f}}, \quad \dot{\boldsymbol{\delta}} = \boldsymbol{0}, \\ \boldsymbol{\omega} = \boldsymbol{\omega}_{\mathrm{f}}, \quad \dot{\boldsymbol{\Omega}} = \boldsymbol{0}. \end{cases}$$

The input constraints caused by the limit of actuators are

$$\begin{cases} |\dot{\delta}_i| < \dot{\delta}_{i\max}, \quad |u_i| < u_{i\max}, \\ |\dot{\Omega}_i| < \dot{\Omega}_{i\max}, \quad |v_i| < v_{i\max}, \end{cases}$$

where $i = 1, 2$.

In fact, Eq. (18) can be generalized as the form below

$$\dot{\boldsymbol{x}}(t) = f_{\mathrm{c}}(\boldsymbol{x}(t), \boldsymbol{u}(t), \boldsymbol{v}(t), \boldsymbol{T}_{\mathrm{ext}}), \tag{19}$$

where $\boldsymbol{x} = (\boldsymbol{q}, \boldsymbol{\omega}, \boldsymbol{\delta}, \dot{\boldsymbol{\delta}}, \boldsymbol{\Omega}, \dot{\boldsymbol{\Omega}})$ stands for state variables. This equation describes the relationship among state variables, disturbances, and system input variables.

The idea of NMPC is exploited in this work for controller design, with the purpose of realizing the process of attitude maneuver fast and accurately. At each sampling instant, the NMPC scheme requires to solve an open-loop optimal control problem using the current system state as the initial value[24–30]. The optimal control problem at the kth sampling instant is formulated as

$$\begin{cases} \min J = \displaystyle\int_{t_k}^{t_k+T} (\|\boldsymbol{x}(t) - \boldsymbol{x}(t)^{\mathrm{ref}}\|_{\boldsymbol{M}}^2 + \|\boldsymbol{u}(t)\|_{\boldsymbol{R}}^2 + \|\boldsymbol{v}(t)\|_{\boldsymbol{S}}^2)\,\mathrm{d}t \\ \qquad\quad + \|\boldsymbol{x}(t_k + T) - \boldsymbol{x}(t_k + T)^{\mathrm{ref}}\|_{\boldsymbol{P}}^2 \\ \text{s.t.} \quad \boldsymbol{x}(t_k) = \overline{\boldsymbol{x}}_0, \\ \qquad \dot{\boldsymbol{x}}(t) = f_{\mathrm{c}}(\boldsymbol{x}(t), \boldsymbol{u}(t), \boldsymbol{v}(t), \boldsymbol{T}_{\mathrm{ext}}), \\ \qquad \bar{\boldsymbol{r}} \geqslant \boldsymbol{r}(\boldsymbol{x}(t), \boldsymbol{u}(t)), \\ \qquad \overline{\boldsymbol{r}}_{\mathrm{f}} \geqslant \boldsymbol{r}_{\mathrm{f}}(\boldsymbol{x}(t_0 + T)), \\ \qquad \forall t \in [t_k, t_k + T], \end{cases} \tag{20}$$

where $\boldsymbol{P}$, $\boldsymbol{M}$, $\boldsymbol{R}$, and $\boldsymbol{S}$ are the weighting matrices of appropriate dimension, T is the length of the predictive horizon, $\bar{\boldsymbol{x}}_0$ is the measurement of the system state at the sampling instant, $\boldsymbol{u}\,(t)$ and $\boldsymbol{v}\,(t)$ stand for control input vectors, $\boldsymbol{r}_{\mathrm{c}}$ and $\boldsymbol{r}_{\mathrm{f}}$ denote the path and terminal constraints, respectively, and $\boldsymbol{x}\,(t)$ and $\boldsymbol{x}\,(t)^{\mathrm{ref}}$ are the state at the time instant t and its reference value, respectively. The integrant in the cost function J is taken to be the sum of the squares of the control inputs and the state errors with respect to the reference values, with the purpose of minimizing tracking errors and control efforts. Besides, the cost function also includes a terminal term to penalize the state errors at the ending time.

For numerically solving the optimal control problem defined by Eq. (20), the multiple shooting method in Ref. [29] is used to transform and solve the continuous optimal control problem. Detailed information about the multiple shooting method can be found in Ref. [29]. Notably, the continuous-time differential equation, i.e., Eq. (19), is discretized using the following 4-stage explicit Runge Kutta (ERK) method such that

$$\begin{cases} \boldsymbol{K}_1 = f_{\mathrm{c}}(t_n, \boldsymbol{x}_n, \boldsymbol{u}_n, \boldsymbol{v}_n), \\ \boldsymbol{K}_2 = f_{\mathrm{c}}\Big(t_n + \dfrac{\delta_{\mathrm{s}}}{2}, \boldsymbol{x}_n + \dfrac{\delta_{\mathrm{s}}}{2}\boldsymbol{K}_1, \boldsymbol{u}_n, \boldsymbol{v}_n\Big), \\ \boldsymbol{K}_3 = f_{\mathrm{c}}\Big(t_n + \dfrac{\delta_{\mathrm{s}}}{2}, \boldsymbol{x}_n + \dfrac{\delta_{\mathrm{s}}}{2}\boldsymbol{K}_2, \boldsymbol{u}_n, \boldsymbol{v}_n\Big), \\ \boldsymbol{K}_4 = f_{\mathrm{c}}(t_n + \delta_{\mathrm{s}}, \boldsymbol{x}_n + \delta_{\mathrm{s}}\boldsymbol{K}_3, \boldsymbol{u}_n, \boldsymbol{v}_n), \\ \boldsymbol{x}_{n+1} = \boldsymbol{x}_n + \dfrac{\delta_{\mathrm{s}}}{6}(\boldsymbol{K}_1 + 2\boldsymbol{K}_2 + 2\boldsymbol{K}_3 + \boldsymbol{K}_4), \end{cases} \tag{21}$$

where the incremental step δ_{s} is equal to the sampling period. Thus, Eq. (19) can be reformulated as the following discrete form:

$$\boldsymbol{x}_{n+1} = \boldsymbol{x}_n + f_{\mathrm{d}}(\boldsymbol{x}_n, \boldsymbol{u}_n, \boldsymbol{v}_n), \tag{22}$$

where

$$f_{\mathrm{d}}(\boldsymbol{x}_n, \boldsymbol{u}_n, \boldsymbol{v}_n) = \frac{\delta_{\mathrm{s}}}{6}(\boldsymbol{K}_1 + 2\boldsymbol{K}_2 + 2\boldsymbol{K}_3 + \boldsymbol{K}_4). \tag{23}$$

The state variables at the next time instant can be evaluated recursively with respect to the last time instant.

By choosing N_p discrete points over the predictive horizon $[t_k,\ t_k + T]$, the optimal control problem can be converted into the following nonlinear programming problem:

$$\begin{cases} \min J_k = \left\| \boldsymbol{x}_{k+N_p} - \boldsymbol{x}_{k+N_p}^{\mathrm{ref}} \right\|_{\boldsymbol{P}}^2 + \displaystyle\sum_{i=0}^{N_p-1} \left\| \boldsymbol{x}_{k+i} - \boldsymbol{x}_{k+i}^{\mathrm{ref}} \right\|_{\boldsymbol{M}}^2 + \sum_{i=0}^{N_p-1} \left\| \boldsymbol{u}_{k+i} \right\|_{\boldsymbol{R}}^2 \\ \qquad\qquad + \displaystyle\sum_{i=0}^{N_p-1} \left\| \boldsymbol{v}_{k+i} \right\|_{\boldsymbol{S}}^2 \\ \text{s.t.} \quad \boldsymbol{0} = \boldsymbol{x}_k - \overline{\boldsymbol{x}}_0, \\ \qquad \boldsymbol{0} = \boldsymbol{x}_{k+i+1} - f_{\mathrm{d}}\left(\boldsymbol{x}_{k+i}, \boldsymbol{u}_{k+i}, \boldsymbol{v}_{k+i}\right) - \boldsymbol{x}_{k+i}, \\ \qquad \boldsymbol{0} \geqslant \boldsymbol{r}\left(\boldsymbol{x}_{k+i}, \boldsymbol{u}_{k+i}\right) - \bar{\boldsymbol{r}}, \\ \qquad \boldsymbol{0} \geqslant \boldsymbol{r}_{\mathrm{f}}\left(\boldsymbol{x}_{k+N_p}\right) - \bar{\boldsymbol{r}}_{\mathrm{f}}, \\ \qquad i = 0, 1, \cdots, N_p - 1, \end{cases} \tag{24}$$

where N_p is the total number of the time intervals of the predictive horizon, $\bar{\boldsymbol{x}}_0$ is the measurement of the system state at the sampling instant, $\boldsymbol{x}_{k+i}$ and $\boldsymbol{x}_{k+i}^{\mathrm{ref}}$ are the states at the time instant $k+i$ and its reference value, and $\boldsymbol{u}_{k+i}$ and $\boldsymbol{v}_{k+i}$ stand for control input vectors, respectively. The integral part of the objective function J in Eq. (20) is approximated as the sum of the discrete values of the integrand at the nodes for $i = 0, 1, \cdots,\ N_p$. In the NMPC scheme, the predictive horizon keeps moving forward during the process of online control by increasing k by 1 at the end of each sampling interval. The generalized Gauss Newton method is used for solving the NLP problem described by Eq. (23). No fundamentals of this algorithm is discussed here, since it has been widely discussed and well developed[29].

4 Simulation cases

Cite a small agile spacecraft as an example. Its inertial matrix is presented as[30]

$$\boldsymbol{J} = \begin{bmatrix} 103.9 & -1.85 & -0.2 \\ -1.85 & 106.38 & -1.55 \\ -0.2 & -1.55 & 146.82 \end{bmatrix} \mathrm{kg} \cdot \mathrm{m}^2.$$

The initial values of angular velocity, the initial quaternion, and the desired quaternion are provided as follows:

$$\begin{cases} \boldsymbol{\omega}_0 = [0\ \ 0\ \ 0]^{\mathrm{T}}\ \mathrm{rad/s}, \\ \boldsymbol{q}_0 = [0.173\,6\ \ -0.526\,4\ \ 0.263\,2\ \ 0.789\,6]^{\mathrm{T}}, \\ \boldsymbol{q}_{\mathrm{f}} = [1\ \ 0\ \ 0\ \ 0]^{\mathrm{T}}. \end{cases}$$

The parameters and the physical constraints are shown below,

$$\begin{cases} \dot{\boldsymbol{\delta}}_0 = \dot{\boldsymbol{\delta}}_{\mathrm{f}} = [0 \;\; 0]^{\mathrm{T}} \text{ rad/s}, \\ \dot{\delta}_{i\,\max} = 2\,\text{rad/s}, \quad \ddot{\delta}_{i\,\max} = 2\ \text{rad/s}^2, \\ \dot{\Omega}_{i\,\max} = 2\ \text{rad/s}^2, \quad \ddot{\Omega}_{i\,\max} = 2\ \text{rad/s}^3, \end{cases}$$

where $i = 1,\ 2$.

Disturbances are chosen as

$$\begin{cases} T_x = 10^{-5}\,(3\cos(\omega_0 t) + 1)\ \ \mathrm{N \cdot m}, \\ T_y = 10^{-5}\,(1.5\sin(\omega_0 t) + 3\cos(\omega_0 t))\ \ \mathrm{N \cdot m}, \\ T_z = 10^{-5}\,(3\sin(\omega_0 t) + 1)\ \ \mathrm{N \cdot m}. \end{cases}$$

The weight matrices introduced in Eq. (20) are given as follows:

$$\boldsymbol{P} = \begin{bmatrix} 3\,000\boldsymbol{I}_7 & \boldsymbol{0}_{7\times 8} \\ \boldsymbol{0}_{8\times 7} & 30\boldsymbol{I}_8 \end{bmatrix}, \quad \boldsymbol{M} = \begin{bmatrix} 3\,000\boldsymbol{I}_7 & \boldsymbol{0}_{7\times 8} \\ \boldsymbol{0}_{8\times 7} & 30\boldsymbol{I}_8 \end{bmatrix}, \quad \boldsymbol{R} = \boldsymbol{I}_2, \quad \boldsymbol{S} = \boldsymbol{I}_2,$$

where $\boldsymbol{I}_N$ denotes an $N \times N$ identity matrix, and $\boldsymbol{0}_{m\times n}$ denotes an $m \times n$ matrix whose elements are all zero.

The numerical simulation is performed for a period of 40 s. The control horizon is taken as 4 s, and 10 intervals are used for discretization over the control horizon. The simulation results are summarized in Figs. 2–11.

Figures 2 and 3 show the time responses of the attitude and angular velocity under the controller based on the NMPC. The spacecraft is stabilized to the desired attitude within 40 s. The magnitudes of angular velocity are smaller than 0.4 rad/s during the total process of maneuver.

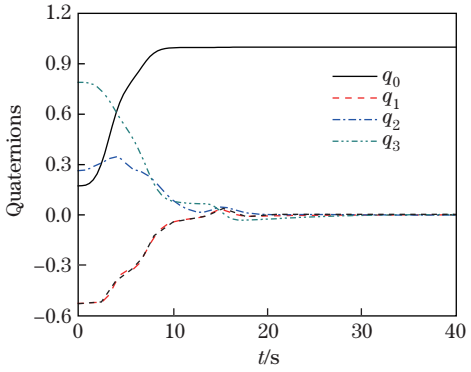

Fig. 2 Time histories of attitude quaternions

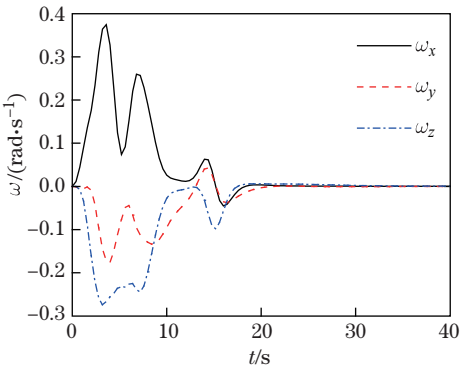

Fig. 3 Time histories of angular velocity

Figures 4–7 show that, VSCMGs can adjust gimbal angles and rotor spinning rates along with system input variables and produce output torques, to make the spacecraft achieve the

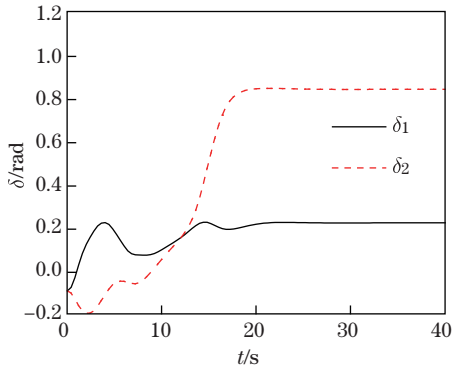

Fig. 4 Time histories of gimbal angles of VSCMGs

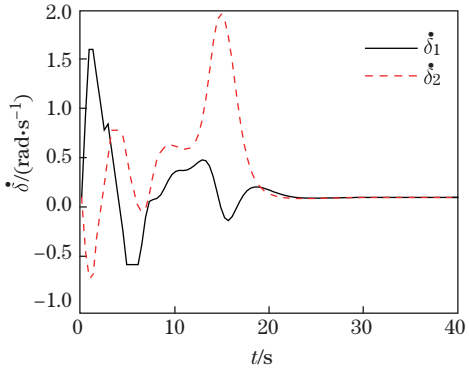

Fig. 5 Time histories of gimbal rates of VSCMGs

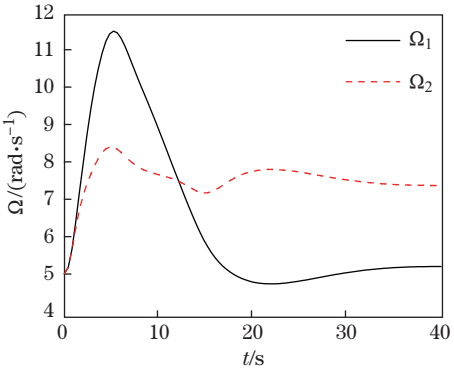

Fig. 6 Time histories of rotor spinning rates of VSCMGs

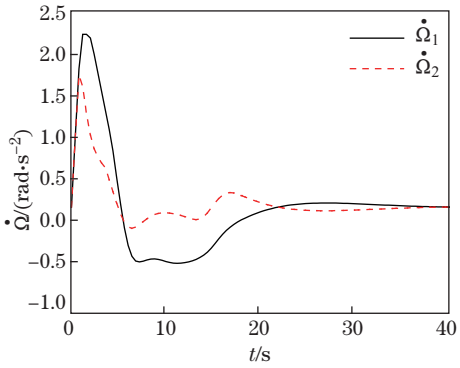

Fig. 7 Time histories of rotor spinning accelerations of VSCMGs

desired attitude and angular velocity. The gimbal rates $\dot{\boldsymbol{\delta}}$ and rotor spinning accelerations $\dot{\boldsymbol{\Omega}}$ will converge to zero without exceeding the amplitudes caused by physical constraints.

Figures 8 and 9 show input variables $\ddot{\boldsymbol{\delta}}$ and $\ddot{\boldsymbol{\Omega}}$ of the system planned by the NMPC method, i.e., $\boldsymbol{u}$ and $\boldsymbol{v}$. $\ddot{\boldsymbol{\delta}}$ and $\ddot{\boldsymbol{\Omega}}$ can achieve the required terminal state in the end without exceeding the amplitudes caused by physical constraints.

Figures 10 and 11 show the total angular momentum and output torques produced by VSCMGs during the spacecraft maneuver. The magnitudes of output torques are kept within the range of 12 N·m. Since the spacecraft and the array of VSCMGs are treated as a whole system, there is no error between output torques of the array of VSCMGs and the demanded torques. After 20 s, the total angular momentum keeps constant, while output torques converge to zero.

To compare with the simulation results obtained by using the proposed strategy, the results of the conventional control strategy are illustrated next in Figs. 12–16. As shown in Figs. 13–16, the RW mode is employed, while the gimbal angles of VSCMGs remain constant. Figures 12–16 illustrate that the whole process of the attitude maneuver based on the conventional steering law can be accomplished within 30 s, a little shorter than that based on the proposed strategy. However, the magnitudes of demanded control torques and state variables such as $\boldsymbol{\delta}, \dot{\boldsymbol{\delta}}, \boldsymbol{\Omega}$, and $\dot{\boldsymbol{\Omega}}$ are significantly higher than those obtained by using the proposed strategy. Furthermore, those state variables drastically change at the beginning of the control process of the conventional method, which may bring great difficulties to the physical realization of VSCMGs.

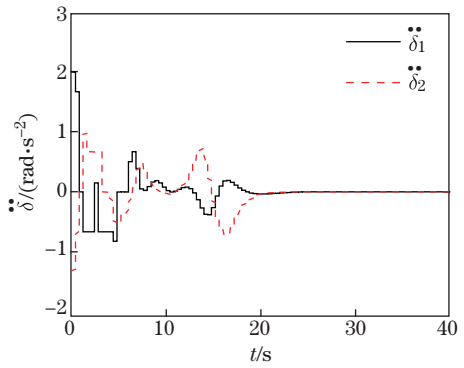

Fig. 8 Time histories of control inputs $\ddot{\delta}_1$ and $\ddot{\delta}_2$

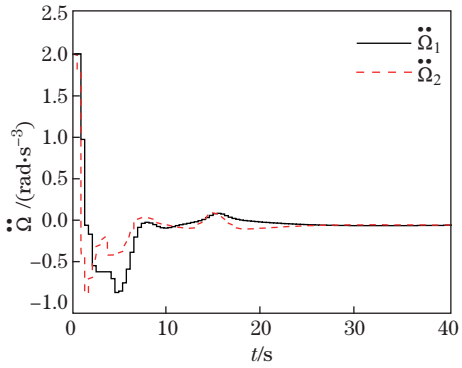

Fig. 9 Time histories of control inputs $\ddot{\Omega}_1$ and $\ddot{\Omega}_2$

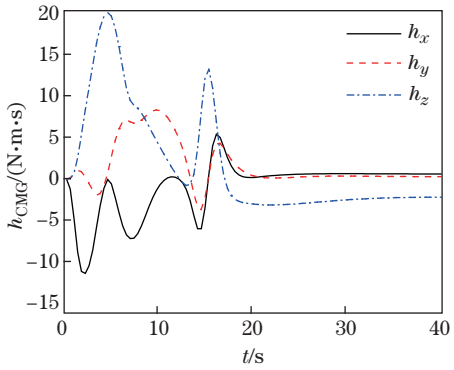

Fig. 10 Total angular momentum of array of VSCMGs

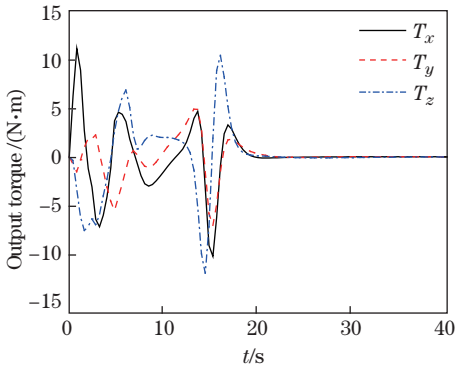

Fig. 11 Output torques produced by array of VSCMGs

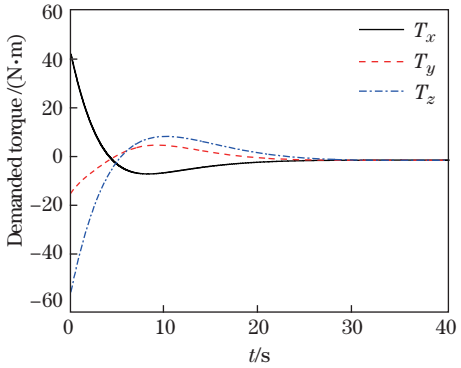

Fig. 12 Demanded control torques based on steering laws

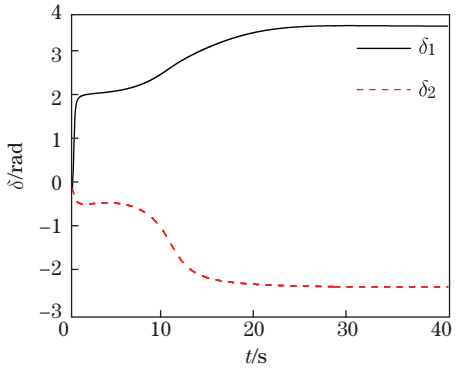

Fig. 13 Gimbal angles of VSCMGs based on steering laws

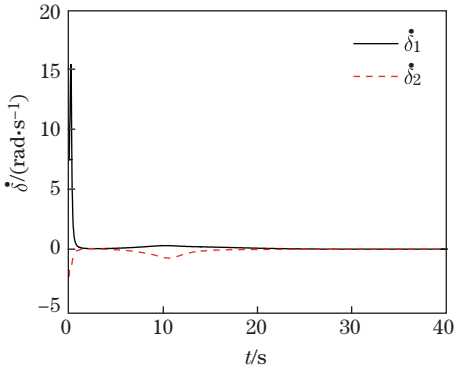

Fig. 14 Gimbal rates of VSCMGs based on steering laws

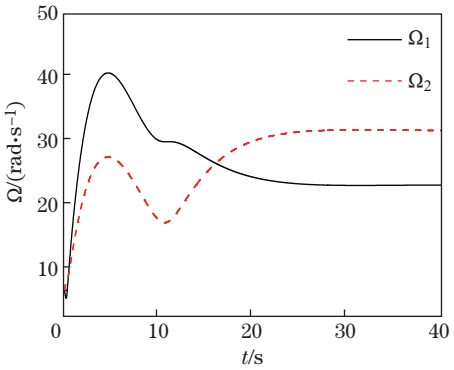

Fig. 15 Rotor spinning rates of VSCMGs based on steering laws

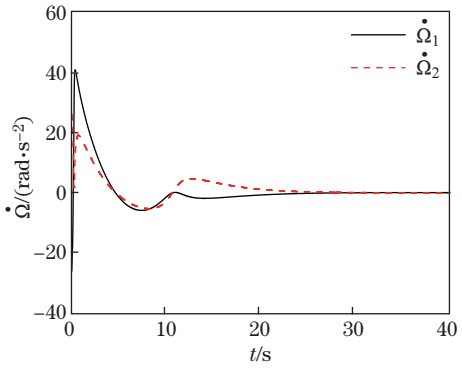

Fig. 16 Rotor spinning accelerations of VSCMGs based on steering laws

5 Conclusions

This paper focuses on the problem of attitude control regarding the rigid spacecraft where the VSCMGs are used as actuators. Firstly, a mathematical model is built by treating the spacecraft and the array of VSCMGs as an entire system and taking the coupling interaction between the spacecraft and VSCMGs into account. Then, the first-order derivative of gimbal rates and the second-order derivative of rotor spinning velocity are treated directly as input variables. Consequently, the explicit treatment of the singularity of CMGs becomes not necessary any more. With the existence of disturbances, the attitude maneuver controller for the spacecraft is designed based on the NMPC method. Compared with the conventional method based on the steering law, simulation results of the proposed strategy demonstrate that, the spacecraft can achieve the desired attitude and angular velocity under the physical restrictions within 40 s smoothly, keeping in view the high precision and stability of orientation. Meanwhile, the system input variables prepared by the controller always satisfy the physical restrictions.

References

[1] Guo, Y. N., Li, C. J., Zhang, Y. H., and Ma, G. F. Spacecraft attitude maneuver using control moment gyroscope with gimbal angle constraints. *Acta Aeronautica et Astronautica Sinica*, **32**(7), 1231–1239 (2011)

[2] Hu, Q., Jia, Y. H., and Xu, S. J. Dynamics and vibration suppression of space structures with control moment gyroscopes. *Acta Astronautica*, **96**(4), 232–245 (2014)

[3] Cheng, G. D. *Research on Attitude Maneuver Control of Agile Satellites Using Control Moment Gyroscope* (in Chinese), M. Sc. dissertation, Harbin Institute of Technology, 60–88 (2014)

[4] Wei, D. Z., Li, G., Fu, R., Wu, D. Y., and Zhang, J. Y. Design of SGCMG and long life rotor bearing system technology in Tiangong-1 (in Chinese). *Science in China* (*Series E*: *Technological Sciences*), **44**(3), 261–268 (2014)

[5] Zhang, J. R. Steering laws analysis of SGCMGs based on singular value decomposition theory. *Applied Mathematics and Mechanics* (*English Edition*), **29**(8), 1013–1021 (2008) DOI 10.1007/s10483-008-0805-2

[6] Wie, B. Singularity analysis and visualization for single-gimbal control moment gyro systems. *Journal of Guidance*, *Control*, *and Dynamics*, **27**(2), 271–282 (2004)

[7] Zhang, J. W., Ma, K. M., and Meng, G. Z. Modeling of spacecraft attitude systems with single gimbal control moment gyros and controllability analysis (in Chinese). *Systems Engineering and Electronics*, **34**(4), 761–766 (2012)

[8] Ford, K. A. and Hall, C. D. Flexible spacecraft reorientations using gimbaled momentum wheels. *Advances in the Astronautical Sciences*, **97**(3), 1895–1914 (1998)

[9] Schaub, H., Vadali, S. R., and Junkins, J. L. Feedback control law for variable speed control moment gyros. *Journal of the Astronautical Sciences*, **46**(3), 307–328 (1998)

[10] Schaub, H. and Junkins, J. L. Singularity avoidance using null motion and variable-speed control moment gyros. *Journal of Guidance*, *Control*, *and Dynamics*, **23**(1), 11–16 (2000)

[11] Cui, P. L. and He, J. X. Steering law for two parallel variable-speed double-gimbal control moment gyros. *Journal of Guidance*, *Control*, *and Dynamics*, **37**(1), 350–359 (2013)

[12] Kanzawa, T., Haruki, M., and Yamanaka, K. Steering law of control moment gyroscopes for agile attitude maneuvers. *Journal of Guidance*, *Control*, *and Dynamics*, **39**(4), 952–962 (2016)

[13] Bhat, S. P. and Tiwari, P. K. Controllability of spacecraft attitude using control moment gyroscopes. *IEEE Transactions on Automatic Control*, **54**(3), 585–590 (2009)

[14] Zhang, J. W., Ma, K. M., Meng, G. Z., and Tian, S. Spacecraft maneuvers via singularity-avoidance of control moment gyros based on dual-mode model predictive control. *IEEE Transactions on Aerospace and Electronic Systems*, **51**(4), 2546–2559 (2015)

[15] Gui, H. C., Jin, L., and Xu, S. J. Maneuver planning of a rigid spacecraft with two skew control moment gyros. *Acta Astronautica*, **104**(1), 293–303 (2014)

[16] Crouch, P. Spacecraft attitude control and stabilization: applications of geometric control theory to rigid body models. *IEEE Transactions on Automatic Control*, **29**(4), 321–331 (1984)

[17] Hu, B. and Ge, X. S. Nonlinear control of attitude stabilization of an underactuated spacecraft (in Chinese). *Journal of Beijing Institute of Machinery*, **24**(1), 12–16 (2009)

[18] Yang, H. and Wu, Z. Attitude controller design of underactuated spacecraft with two control moment gyroscopes (in Chinese). *Proceedings of the 6th World Congress on Intelligent Control and Automation*, IEEE, Dalian, 939–943 (2006)

[19] Chen, L. Q. and Xue, Y. *Theoretical Mechanics* (in Chinese), 2nd ed., Tsinghua University Press, Beijing, 360–389 (2014)

[20] Cui, W. Q. *Research on Attitude Maneuver of Agile Satellites Using SGCMGs* (in Chinese), M. Sc. dissertation, Harbin Institute of Technology, 60–89 (2010)

[21] Di Gennaro, S. Passive attitude control of flexible spacecraft from quaternion measurements. *Journal of Optimization Theory and Applications*, **116**(1), 41–60 (2003)

[22] Wen, H., Chen, T., Jin, D. P., and Hu, H. Y. Passivity-based control with collision avoidance for a hub-beam spacecraft. *Advances in Space Research*, **59**(1), 425–433 (2017)

[23] Hu, Q. and Zhang, J. R. Attitude control and vibration suppression for flexible spacecraft using control moment gyroscopes. *Journal of Aerospace Engineering*, **29**(1), 15–27 (2015)

[24] Wen, H., Zhu, Z. H., Jin, D. P., and Hu, H. Y. Model predictive control with output feedback for a deorbiting electrodynamic tether system. *Journal of Guidance*, *Control*, *and Dynamics*, **39**(10), 2455–2460 (2016)

[25] Peng, H. J. and Jiang, X. Nonlinear receding horizon guidance for spacecraft formation reconfiguration on libration point orbits using a symplectic numerical method. *ISA Transactions*, **60**, 38–52 (2016)

[26] Li, M. W. and Peng, H. J. Solutions of nonlinear constrained optimal control problems using quasilinearization and variational pseudospectral methods. *ISA Transactions*, **62**, 177–192 (2016)

[27] Wen, H., Zhu, Z. H., Jin, D. P., and Hu, H. Y. Tension control of space tether via online quasilinearization iterations. *Advances in Space Research*, **57**(3), 754–763 (2016)

[28] Li, P., Zhu, Z. H., and Meguid, S. A. State dependent model predictive control for orbital rendezvous using pulse-width pulse-frequency modulated thrusters. *Advances in Space Research*, **58**(1), 64–73 (2016)

[29] Quirynen, R., Vukov, M., Zanon, M., and Diehl, M. Autogenerating microsecond solvers for nonlinear MPC: a tutorial using ACADO integrators. *Optimal Control Applications and Methods*, **36**(5), 685–704 (2015)

[30] Fan, G. W., Chang, L., Dai, L., Xu, K., and Yang, X. B. Nonlinear model predictive control of agile satellite attitude maneuver (in Chinese). *Optics and Precision Engineering*, **23**(8), 2318–2327 (2015)